# THEORETICAL AND EXPERIMENTAL MESOSCALE STUDIES OF IMPACT-LOADED GRANULAR EXPLOSIVE AND SIMULANT MATERIALS

M. R. Baer and W. M. Trott
Engineering Sciences Center
Sandia National Laboratories*, Albuquerque, NM, 87185

Three-dimensional numerical simulations and line-imaging optically recorded velocity interferometer measurements are used to investigate the mesoscale response of impact on granular sugar and low-density HMX. Spatially resolved measurements of transmitted waves demonstrate a strong correlation between the particle distribution and the amplitude/frequency of the fluctuating fields as revealed by wavelet analysis. At conditions near the onset of reaction, the resulting wave fields indicate that energy release evolves as a complex stochastic process.

Detailed wave fields from numerical mesoscale simulations are probed using imaging and averaging techniques to determine statistical and mean properties of the shock fields. These methods provide the temporal and spatial variations of probabilistic distribution functions (PDF) of various wave fields that are key toward understanding the initiation and growth states of reaction in heterogeneous materials. Analysis of thermal fields has identified four aspects of the shock response associated with elastic-to-plastic deformation, bulk loading, thermal gradients and 'hot-spot' localization effects. Similar methods have also been applied to determine the variations of kinetic energy states and stress-strain distributions associated with the dispersive waves produced by shock loading the heterogeneous material. These new insights suggest that reactive waves are distinctly different than the traditional models based on singular jump state analysis and new directions based on PDF theory have been identified to link the mesoscale information to the continuum-level.

## INTRODUCTION

At the mesoscale, the shock behavior of heterogeneous materials consists of multiple waves that interact with material heterogeneities or internal boundaries. In energetic materials, the processes occurring at the grain or crystal level[1] control the shock sensitivity of initiation and sustained reaction. An ensemble of crystals and/or binder materials can interact to cause fluctuations of the thermodynamic fields and localization of energy to trigger reaction.

In heterogeneous materials, the shock wave fields are three-dimensional and unsteady arising first at contact points then coalescing to produce a distribution of thermal and mechanical states. If the loading is sufficient to cause plastic deformation, internal boundaries fold and form micro-jets during compaction. When averaged over a sufficiently large space, a "shock" in heterogeneous material appears to be dispersive and dissipative. Rather than a single jump state, the consolidated material consists of a distribution of fluctuating states spanning a broad range of length and time scales. Much of this multiscale behavior appears similar to the nature of fluid turbulence whereby the redistribution of kinetic energy occurs due to interactions of stochastic microstructure.

Although direct numerical simulations of the shock loading of heterogeneous materials have revealed various features of the wave fields, much of this new information has yet to be incorporated at the continuum level. To achieve this goal, data interrogation techniques are devised to probe the vast quantity of four-dimensional data from detailed numerical simulations. In this work, image-processing software is used to extract statistical properties of the shock field states during loading of heterogeneous material.

Experimental characterization of the shock response of these materials at the requisite scale lengths can in turn provide much useful information for validation and calibration of the numerical models. Unlike numerical simulations, the line-imaging

* Sandia is a multiprogram laboratory operated by Sandia Corporation, a Lockheed Martin Company, for the U.S. Department of Energy under contract DE-AC04-94AL85000.

velocity interferometry measurements described in this work are not able to address directly many of the details of wave interactions within the heterogeneous sample. Rather, this diagnostic probes temporal and spatial variations in the transmitted wave behavior at a boundary. Important features of the wave profile may relate to parameters such as sample geometry, particle size distribution and particle morphology. In particular, the experiments can provide information on temporal effects (wave speeds and rise times), particle velocities including spatial (transverse) variations, and ordered structures (e.g., fluctuations with characteristic frequencies). Results are amenable to characterization using statistical methods as well as techniques for scale-dependent (e.g., wavelet) and stationary wave analysis. Statistically significant variations in the wave profile as a function of impact velocity, sample thickness, and sample particle size distribution, etc. establish useful constraints for the mesoscale modeling.

In this paper, we describe experiments designed to explore the mesoscopic scale response of a common secondary explosive (HMX) in comparison with that of granulated sugar (sucrose), an inert explosive simulant. These tests both directly compare to and expand on a series of magnetic gauge studies of low-density sugar and HMX performed by Sheffield, et al.[2,3] Experiments on low-density, porous sugar address mesoscopic scale thermomechanical effects in the absence of rapid reaction. The sugar experiments described here focus on the dispersive wave behavior as a function of impact velocity, sample thickness and particle size distribution. The tests on HMX begin to address the complex, additional effects of chemical reaction in the shock response.

## IMPACT EXPERIMENTS

Simultaneous line-imaging ORVIS and single-point VISAR measurements have been made on waves transmitted by pressed sugar (2.27-mm to 6.16-mm thick) and HMX samples (4-mm thick) in a gas gun target design very similar to that used in the previous magnetic gauge studies[2,3]. A schematic diagram of this design is shown in Figure 1. The target assembly consists of a Kel-F impactor and a Kel-F target cup containing sugar or HMX pressed to 65% theoretical maximum density (TMD). A 0.225-mm-thick buffer layer of Kapton and an aluminized PMMA interferometer window confines the porous bed. The buffer is used to mitigate the loss in reflected light intensity that typically occurs upon shock arrival at the window. To achieve consistency in preparation of the low-density, porous samples, both mass and volume of the material were carefully controlled.

Most sugar samples were prepared directly from coarse, granulated material. The measured particle size distribution (as received and after pressing) has been reported previously as given in Reference 4. The largest weight fraction (~60%) of the granulated sugar resides in a grain size range of 250-425µm. A significant amount of grain crushing occurs even at the low pressing density used in this study. Additional sugar samples were prepared from sieved material in the following ranges: 106-150µm, 150-212µm, 212-300µm, and 250-425µm. HMX samples were prepared from three different materials: [1] a coarse-grained lot of Holston batch HOL 920-32 (mean particle size near 120µm), [2] a fine-grain sieved sample (38-45µm), and [3] a coarse-grain sieved sample (212-300µm).

The line-imaging ORVIS used in this study is a compact system that combines the interferometer optics, laser source (2W $NdYVO_4$ CW laser), and streak camera/intensifier/CCD detector on a single 2' x 6' optical breadboard. Detailed discussions of the instrumentation, the optical coupling to the gas gun target chamber, and image data reduction methods are described in Reference 4. Single-point VISAR data were obtained using a dual-delay-leg, "push-pull" assembly.

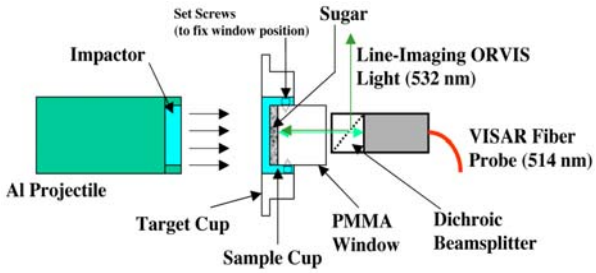


**FIGURE 1.** Schematic diagram of gas gun target design for measurements on low-density sugar or HMX.

## MESOSCALE MODELING

In simulating the aforementioned gas-gun experiments, detailed 3-D numerical simulations of randomly packed crystal ensembles subjected to shock loading are conducted using the Eulerian shock physics code, CTH[5]. Included in these computations are the effects of material strength and thermal dissipation. The details associated with the particle-packing algorithm, material models and boundary conditions are given in Reference 6 and not repeated here.

Granular sugar is represented as a collection of crystals with a prescribed unpressed particle size distribution consisting of eight classes of particle size. A closely packed geometry is created using a MC/MD method forming an initial configuration with a porous density of ~65% TMD. Incorporated into the computational model are the Kapton and PMMA layers of the gauge package used in the gas gun impact experiments.

The physical domain of the computations was defined to be large enough to capture statistical averages. To that end, the lateral width of the granular layer is reduced so that an overall length scale is approximately eight mean particle diameters ($d_m$ ~120 μm) that should be sufficient for a statistical average. Thus, approximately five hundred crystals form the entire geometry and periodic conditions are imposed at the lateral boundaries. A reverse ballistic condition imposes an initial velocity on the ensemble relative to the impact surface. A shock load is then produced in the granular material as it stagnates at the rigid wall boundary. Tracers at the Kapton/PMMA interface are included to monitor the particle velocities at a location corresponding to the probe region of the line-imaging interferometer.

All of the relevant material parameters for the granular sugar are given in Table 1. The Kapton and PMMA materials of the gauge package are modeled with Mie-Grüneisen equation of state using the CTH EOS database parameters. The numerical resolution is fixed at a uniform cell size of 2μm requiring 120 million cells in the computations. These simulations were conducted on the ASCI-Red TFLOPS computer using 256 processors.

Figure 2 displays an initial 3D material geometry of the ensemble of sugar crystals at the impact condition of 370 m/s. (The pore regions of the initial granular material are assumed to be void.) Details of the simulation show that localization effects first occur at contact points and subsequently, plastic flow into the interstitial pores produces localized regions of elevated temperature. Eventually, multiple shocks interact with the gauge package producing reflected and transmitted waves at the gauge/crystal ensemble interface location.

## SUGAR EXPERIMENTS

As described previously,[4] results from both VISAR and line-imaging ORVIS are generally consistent with the systematically varying dispersive behavior of wave profiles vs. impact velocity reported by Sheffield, et al.[2] We present here some representative results that illustrate aspects of the complex wave behavior for different sample conditions. This includes a direct comparison between

**Table 1**. Granular Sugar EOS/Strength/Fracture Parameters

| Parameter | Value |
|---|---|
| Particle Size Dist.<br>46 μm<br>64 μm<br>91 μm<br>116 μm<br>138 μm<br>181 μm<br>231 μm<br>338 μm | Wt. & # fraction:<br>0.005, 0.265<br>0.008, 0.148<br>0.020, 0.133<br>0.021, 0.068<br>0.058, 0.111<br>0.165, 0.139<br>0.152, 0.062<br>0.571, 0.074 |
| Crystal Density - $\rho_o$ | 1.5805 g/cm$^3$ |
| Sound Speed - $c_o$ | $3.04\times10^5$ cm/s |
| Slope of $U_s$-$U_p$ - $s$ | 2.05 |
| Grüneisen - $\Gamma_o$ | 1.04 |
| Specific Heat - $c_v$ | $1.38\times10^{11}$ erg/gm-ev |
| Thermal Cond. - $\lambda_s$ | $4.86\times10^8$ erg/cm$^2$-s-ev |
| Yield Stress - $Y$ | 1.1 Kbar |
| Poisson Ratio -ν | 0.25 |
| Fracture Stress - $\sigma_f$ | -2.0 Kbar |

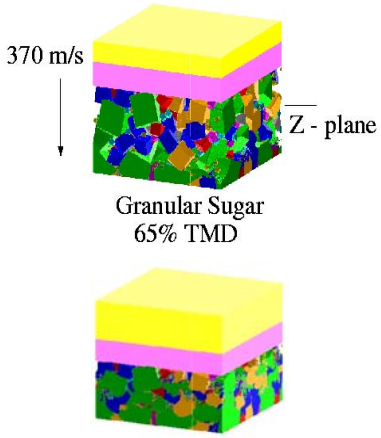


**FIGURE 2**. The initial 3D materials used in the numerical simulation of the granular sugar impact tests and pictorial of ensemble 1000 ns after initial impact at 370 m/s

the observed wave profiles and those determined by the three-dimensional simulations.

In the numerical simulation illustrated below, particle velocity were recorded at approximately 50 "tracer" points along a line segment located at the Kapton/ PMMA interface. The velocity-time profile is shown in Fig. 3a. A spatially resolved velocity-time plot from line-imaging ORVIS data [7] obtained using a similar sample geometry and particle size distribution is presented in Figure 3b. The simulations and experimental measurements both exhibit a ramp wave (~100-150 ns duration) preceded by a low-amplitude precursor. The late-time velocities are also very similar (~0.25 km/s). Significant longitudinal and transverse wave structures are also apparent in both cases. The detailed structure is highly statistical in nature; significant variation in the amplitude and distribution of the fluctuations has been observed experimentally (i.e., shot-to-shot). The agreement between the simulations and the experimental measurements is reasonably good considering that the granular geometry is ideally represented as a randomly packed ensemble of cubic "crystals". Much of the late time response observed experimentally is suspected to be due to viscoelastic response of the window materials not treated in the simulation. Both experiments and computations indicate that the shock response of the heterogeneous material consist of multiple waves rather than a single jump state.

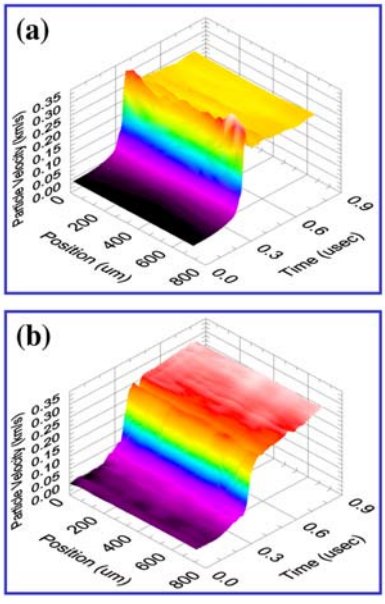


**FIGURE 3.** Comparison of (a) predicted and (b) measured velocity profile of wave transmitted by 2.27-mm-thick sugar sample at an impact velocity of 0.5

## NUMERICAL DATA INTERROGATION

Although the detailed particle velocity line-image ORVIS measurements provide insightful information on transmitted wave behavior, the technique does not reveal the complete picture of the shock response. Details of the simulations show that within the ensemble of granular material multiple shocks are produced containing important statistical information related to the fluctuating thermal and mechanical states. Interrogating the massive quantity of numerical data in transient three-dimensional computer simulations is a computationally intensive task; thus a method had to be devised to data-mine this information.

In this study, image-processing software, such as Image-Pro Plus[8], is used to extract the statistical information relevant for averaging and filtering the fields needed for developing improved continuum-level models of shocked heterogeneous materials.

Four-dimensional data is first rendered as planes of gray-scale contours. As an example, consider the field of temperatures from a direct numerical simulation as displayed in Figure 4. The gray scales of temperature contours are shown for a cross-section plane transverse to the impact direction at a time when the waves have penetrated into the gauge package.

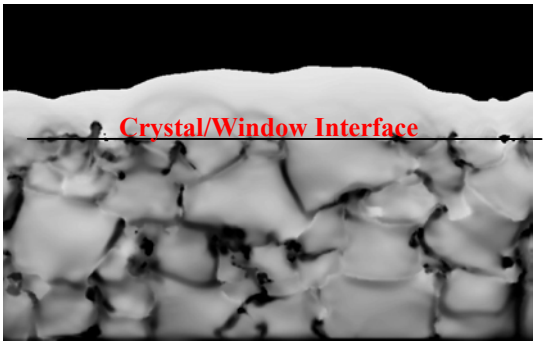


**FIGURE 4**. Gray-scale contours of the temperature field at the midplane of the ensemble transverse to the impact direction.

The spatial and temporal image planes of information contain 256 levels of pixel intensities spanning a linear range of temperatures. A pixel count per gray-scale intensity yields the distribution of states. This information is directly related to a probability distribution function (PDF). Furthermore, the set of spatial or temporal cut planes is the basis for an ensemble average of the PDF.

Various parts of the PDF can be masked to identify characteristics of the field of interest. Then, image data is sampled to assemble relevant statistics such as mean size, area, fractal dimension, etc.

Figure 5 displays an overlay of the temperature PDF's from 150 transverse cut planes in the crystal ensemble 800 ns after initial impact. Four divisions of the temperature distribution are identified as illustrated in Figure 6: I - a precursor range associated with elastic stress waves, II - bulk response in which much of the mechanical load is supported, III - a thermal gradient range near grain boundaries and IV - the tail portion of the distribution associated with the localization of energy into "hot-spots". For reactive materials, region IV serves as the centers of first reaction and region III is the range associated with the growth of reaction.

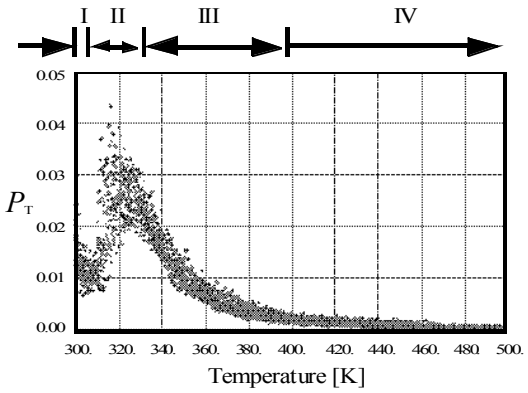


**FIGURE 5**. Representative temperature PDF's displaying the four ranges of the temperature field.

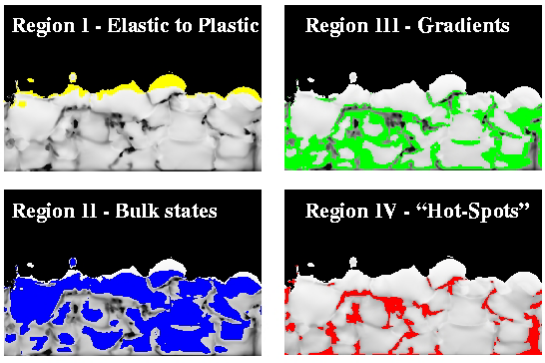


**FIGURE 6**. Masked regions of the various parts of the temperature distribution

Having identified the various aspects of the temperature PDF, masks of each of the four parts are superimposed on the contour images, separated from the original image and the statistics are re-sampled. Figure 7 displays the time evolution of the volume fraction of shocked material corresponding to each part of the temperature distribution function. At this impact condition, roughly 10% of the material contains localized high temperatures forming "hot-spots". The gradient range represents approximately 25% of the solid volume fraction, hence, the sum of the two parts of the distribution displaces a volume corresponding to that of the initial porosity.

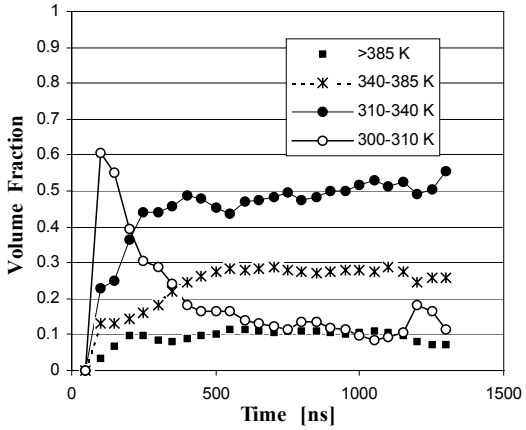


**FIGURE 7**. Ensemble-averaged volume fraction for each region of the temperature distribution.

A somewhat different view of the temperature PDF arises if the field is sampled along the impact direction. In this case, the distribution of the temperature field corresponds to a fixed time and the cut planes from the impact surface are probed. Figure 8 displays an overlay of temperature distributions at various z-planes 800 ns after initial impact.

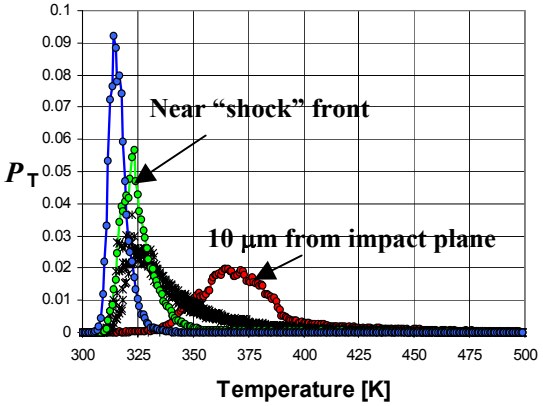


**FIGURE 8**. The spatial variation of the temperature PDF at 800 ns after initial impact.

Near the initial impact plane the temperature distribution is Gaussian with a higher mean temperature than the fields within the compacted ensemble. As the waves move deeper into the heterogeneous material the temperature field approaches a Maxwellian distribution. Near the gauge window the temperature field is nearly uniform corresponding to conditions of the elastic precursor region and represented as a delta function. The implication of this result suggests that temperature measurements at an impact surface or near a window interface may not be indicative of the localized fields within the shocked heterogeneous material. Different distributions are seen at both the impact and gauge surfaces.

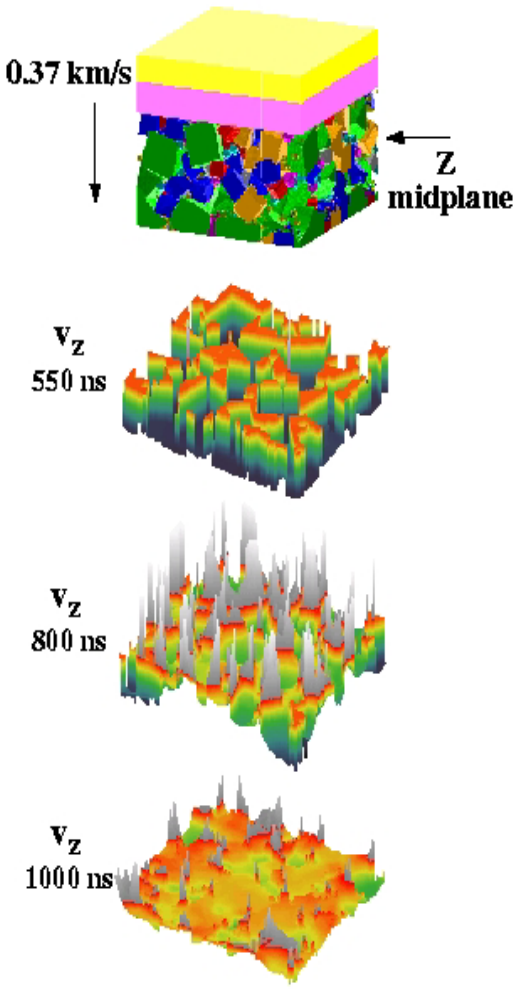


**FIGURE 9**. Temporal variations of the z-velocity component at the midplane of the crystal ensemble.

In addition to investigating the stochastic scalar fields, such as temperature, the vector and tensor fields are also expected to be distributed states. The same type of data interrogation is applied to the velocity components to determine how kinetic energy is redistributed during shock loading.

Figure 9 illustrates the temporal variations of the z-component of the velocity field (in the impact direction). These variations correspond to the midplane in the ensemble and are displayed at various times as the shocks pass through this location. Prior to 500 ns, the velocity is constant with no crystal interactions at the midplane location. The "valleys" of the surface plots correspond to the void regions. Variations in excess of the impact velocity are rendered in gray scale. As the shocks begin to interact within the crystal ensemble, large fluctuations occur near the crystal boundaries as material jets into the open pores. This simulation shows that nonuniform material motion persists for a relatively long time. (A uniform equilibrated state corresponds to a plane with no variations.)

**Normal velocity component**

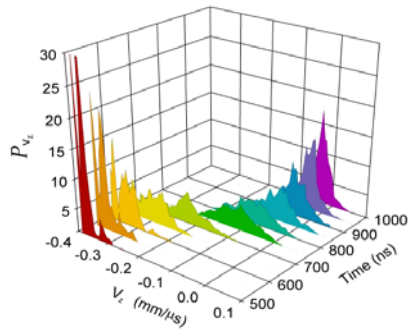


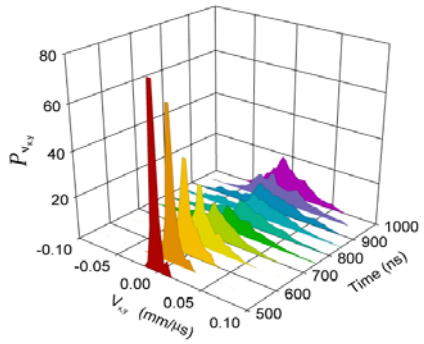


**Transverse velocity component**

**FIGURE 10**. Temporal variations of the material velocity components at the midplane of the ensemble.

To illustrate how kinetic energy is redirected during shock loading, the components of the

material velocity are separated and the distributions are determined by the image-processing technique. Figure 10 displays the temporal variations of the normal and traverse components at the midplane of the ensemble.

Initially, the normal component of material velocity is constant. As the crystals begin to interact, material movement redirects the normal velocity to the transverse components producing Gaussian distribution functions. Eventually, all of the velocity components form a delta distribution as material stagnates relative to the initial impact surface.

Similar data-mining techniques can be applied to the tensor fields such as stress or strain. Consider the volumetric strain field represented by material densities at the midplane section within the shocked ensemble. Initially, the material density of the crystals is constant and its distribution is defined as a delta function. As the shocks pass through the material, variations arise due to the effects of the mechanical and thermal stresses.

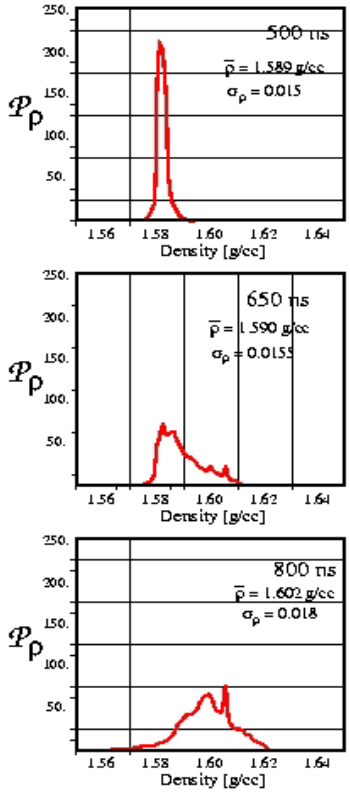


**FIGURE 11**. Temporal variations of the material density at the midplane of the crystal ensemble

Figure 11 displays the PDF for the density field as the shocks pass through the midplane section. The initial delta distribution changes to a Gaussian distribution. These variations appear stationary because localized 'hot spots' induce thermal strains that dissipate slowly by thermal conduction.

Figure 12 displays contours of the pressure and density fields at the midplane of the ensemble 800 ns following initial impact. At the midplane, the first indication of shock behavior appears approximately 500 ns after initial impact, yet 300 ns later, the stress and strain fields remain nonuniform and the shock response is clearly in a state of nonequilibrium. Furthermore, the variations of the strain field are not directly correlated to those of the stress field due to thermal variations that reside at the grain boundaries.

.

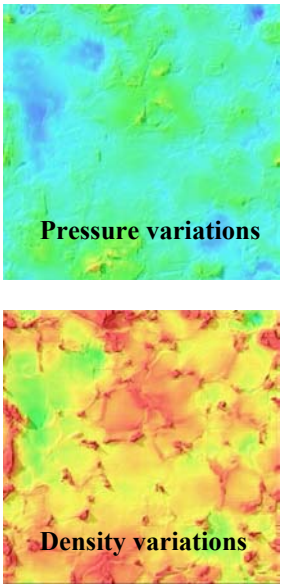


**FIGURE 12**. Variations of pressure and density at the midplane of the crystal ensemble 800 ns after impact.

## A LINK TO THE CONTINUUM

Mesoscale modeling has clearly identified that the thermal and mechanical states associated with impacting a heterogeneous material with stochastic geometry can be well described as distribution of states or PDF's. This suggests a new approach to multiple-scale material modeling linking the mesoscale to continuum level descriptions.

Much of the formalism of PDF methods has been previously developed for the modern theory of turbulence in fluids (see Reference 9). Only the rudimentary aspects of this approach are discussed here.

The set of field variables, $\phi_i$, is represented as distribution states with a probability density function, $P_{\phi_i}$, for each variable such that $\int_0^\infty P_{\phi_i} d\phi_i = 1$. The mean and variance of these variables are defined as:

$$\overline{\phi}_i = \int_0^\infty \phi_i P_{\phi_i} d\phi_i \text{ and } \left\langle \sigma_{\phi_i}^{\ 2} \right\rangle = \int_0^\infty P_{\phi_i} (\phi_i - \overline{\phi}_i)^2 d\phi_i .$$

In the PDF approach, transport relationships for $P_{\phi_i}(\phi_i, t)$ are defined that are functions of space and time as well as being jointly dependent on other field variables. Although PDF transport equations can be fundamentally derived from the conservation equations, a simplified approach can also be based on stochastic differential equations.

Detailed mesoscale simulations provide a determination of $P_{\phi_i}(\phi_i, t)$, and forms of the stochastic "forces" can then be deduced from the transport equations. As a result, the evolution of the state distributions can be projected to the domain boundaries where measurements are typically made. Future work is planned to determine these stochastic relationships.

## LOW-DENSITY HMX EXPERIMENTS

With the added factor of rapid chemical energy release, the behavior of transmitted wave profiles in porous explosives at mesoscopic scales provides a rich area of study. The recent, detailed review by Sheffield et al.[3] on shock loading of porous explosives provides much helpful background information for the work described here. In magnetic gauge studies of low-density (65-74% TMD) HMX, Sheffield et al. have shown that compaction waves at levels below the threshold for reaction in the porous explosive behave in a manner similar to those measured in low-density pressings of sugar. The transmitted waves are spatially and temporally diffuse. At levels above the threshold for initiation, chemical reaction causes the wave to accelerate and to become steeper as it travels. The observed transmitted wave behavior is a complex function of both pressing density and particle size distribution. Consistent with the conventional understanding on explosive sensitivity, HMX pressings at higher density were found to be generally less sensitive. Reaction also occurs at a much lower loading pressure in coarse-grained HMX than in fine-grained HMX. Once reaction is initiated in the fine-grained HMX, however, chemical energy release occurs much more rapidly. These observations support the long-standing qualitative picture of heterogeneous explosive initiation via hot spot formation and grain burning. In coarse materials, hot spots are relatively large and persistent, leading to initiation at low input pressures. In the case of finer materials, hot spots are more numerous but much smaller in size and subject to rapid cooling, resulting in less sensitivity overall. On the other hand, grain-burning models in which the rate of reaction depends on particle size and surface area predict a very rapid reaction growth once reaction begins to spread in the fine-grained explosive.

To explore the effects of initiation and reaction growth at mesoscopic scales in low-density HMX, we have prepared and tested gas gun targets similar to those represented schematically in Figure 1. Transmitted wave behavior has been examined primarily as a function of impact velocity and particle size distribution. Differences in reactivity for three different HMX materials are illustrated in Figure 13. Specifically, this plot shows the decrease in the transit time of the transmitted wave as a function of impact velocity. Lines connecting the various points are only included for visual clarity and are not intended to represent a comprehensive fit to the data. These results are consistent with the grain size effects outlined above. The increase in wave speed for the fine-grain (38-45μm) material is modest and consistent with trends observed in non-reactive sugar pressings. For samples with larger mean particle size, definite wave acceleration occurs (with concomitant increases in particle velocity) as impact velocity increases.

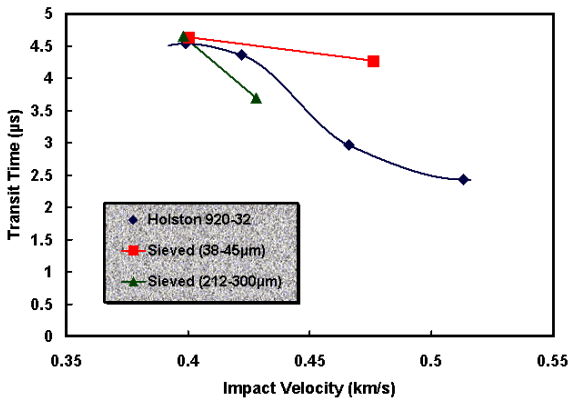


**FIGURE 13.** Transit times for waves transmitted by 4-mm-thick samples of 65% TMD HMX.

Examination of the spatially resolved velocity-time records obtained using line-imaging

ORVIS provides a revealing glimpse of the complexity of chemical energy release on mesoscopic scales. Velocity profiles for the three different HMX materials (at impact velocities near 0.4 km/s) are shown in Figure 14. In the HOL 920-32 sample (mean particle size near 120µm), the transmitted wave is diffuse with a rise time ~150-200 ns, slightly faster than that reported by Sheffield, et al.[3]. Also evident is modest wave growth in localized regions, reflecting the onset of exothermic reaction. This behavior contrasts with wave profiles observed in the fine-grain material (e.g., Figure 14b) that show little or no evidence of chemical energy release. The coarse-grain (212-300µm) material, on the other hand, exhibits substantial wave growth (e.g., Figure 14c—note change in velocity scale).

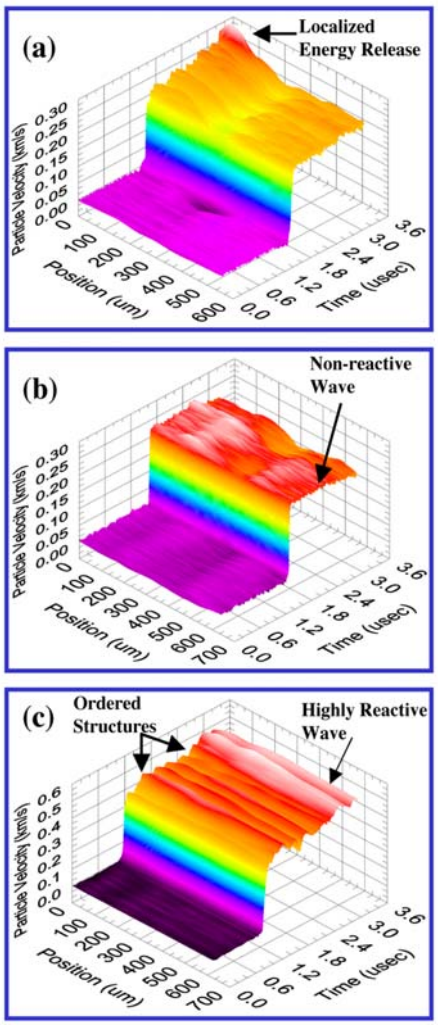


**FIGURE 14**. Transmitted wave profiles from 65% TMD HMX with three different particle size distributions at an impact velocity ~ 0.4 km/s : (a) HOL 930-32—mean particle size ~120µm, (b) Sieved—38-45µm, (c) Sieved—212-300µm

Also evident in this material are ordered wave structures that are distributed over the line segment but are largely coherent temporally.

The distinct response of coarse sieved materials presents especially interesting test cases for validation and refinement of the numerical simulations. Of particular interest as characteristic signatures are the resonance-like fluctuations. Similar wave oscillations are apparent in the wave transmitted by coarse, sieved sugar; however, the fluctuations in porous HMX are better defined and appear to be "chemically amplified." The near periodic nature of these fluctuations is apparent even in single-point measurements such as the VISAR record shown in Figure 15.

While the oscillations are not strictly stationary, FFT analysis identifies a characteristic period near 300ns in this case. This near periodic behavior is clearly apparent in continuous wavelet transforms (CWTs) of both VISAR and line-imaging ORVIS data. A graphical representation of wavelet coefficients from a 1-D CWT (MATLAB® Release 12.1, Wavelet Toolbox) of the VISAR record is shown in Figure 16.

Future work is planned to incorporate HMX chemistry into the detailed 3D numerical mesoscale computation to assess the PDF states associated with reaction. Much uncertainty on the mechanism and reaction rates currently exist that may be applicable to model reactive waves, however, these experiments suggest that reactive behavior must consider the stochastic nature of microstructure.

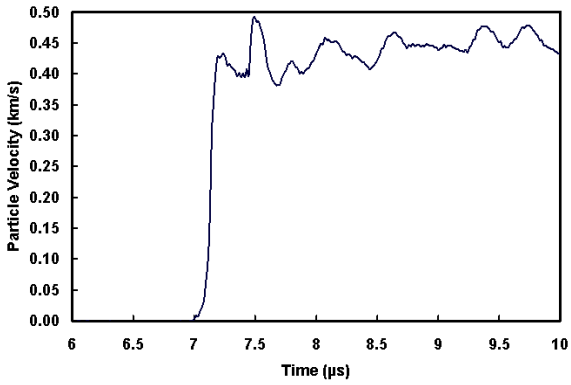


**FIGURE 15.** VISAR record of transmitted wave from sieved HMX (212-300µm); impact conditions are the same as that for Fig. 14c.

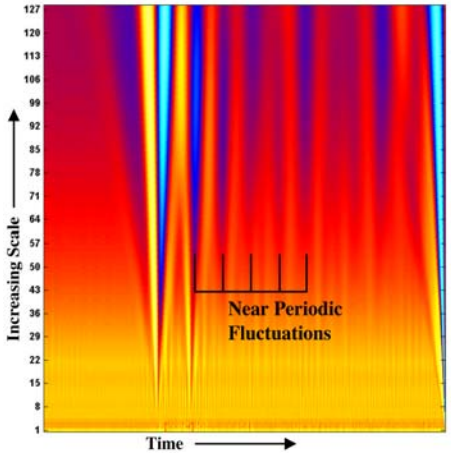


**FIGURE 16.** Graphical representation of wavelet coefficients from 1-D CWT of VISAR data shown above.

## SUMMARY AND CONCLUSIONS

This study has focused on probing experimentally and numerically wave field information to extract statistics associated with shock loaded heterogeneous materials. The ORVIS and VISAR techniques have been used to capture the detailed particle velocities transmitted from a thin layer of granular material.

Image-processing software has been used to data-mine ensembles of contour planes of information from direct numerical simulations. Representative PDF's of temperature have suggested four aspects of the shock response. Additional statistical information has been obtained for other mechanical and thermodynamic fields such as those associated with stress, strain and velocity fluctuations.

Future efforts will explore how these distributions are related to the stochastic geometry and properties of the initial state of the material. Ultimately, this state distribution information will be used in the development for a new approach in modeling shocks in heterogeneous materials.

## ACKNOWLEDGEMENTS

We would like to thank Jaime Castañeda and Lalit Chhabildas for their assistance in the experimental work and David Kethison for his help with the image processing. We also thank Steve Sheffield and Rick Gustavsen (LANL) for much helpful assistance in the experimental design and for sharing their sugar EOS and shock Hugoniot data.

## REFERENCES

1. Bowden, F.P. and Yoffe, A.D., *Initiation and Growth of Explosions in Liquids and Solids*, Cambridge University Press, Cambridge, 1952.
2. Sheffield, S. A., Gustavsen, R. L., and Alcon, R. R., "Porous HMX Initiation Studies--Sugar as an Inert Simulant," in *Shock Compression of Condensed Matter--1997*, edited by S. C. Schmidt et al., AIP Conference Proceedings 429, New York, 1998, pp. 575-578.
3. Sheffield, S. A., Gustavsen, R. L., and Anderson, M. U., "Shock Loading of Porous High Explosives," in *High-Pressure Shock Compression of Solids IV*, edited by L. Davison, et al., New York: Springer-Verlag, 1997, pp. 23-61.
4. Trott, W.M., *et al.*, "Dispersive Velocity Measurements in Heterogeneous Materials," Sandia National Laboratories, SAND2000-3082, December 2000.
5. McGlaun, J.M., Thompson, S.L., and Elrick, M.G., "CTH: A Three-Dimensional Shock Wave Physics Code," *Int. J. Impact Eng.*, Vol. 10, 351-360, 1990.
6. Baer, M. R., Kipp, M. E. and van Swol, F., "Micromechanical Modeling of Heterogeneous Energetic Material", proceedings of the 11th Symposium (International) on Detonation, Snowmass, UT, 1998, pp. 788-797.
7. Trott, W. M., Chhabildas, L. C., Baer, M. R., and Castañeda, J. N., "Investigation of Dispersive Waves in Low-Density Sugar and HMX Using Line-Imaging Velocity Interferometry," in *Shock Compression of Condensed Matter--2001*, edited by M. D. Furnish .
8. Image-Pro Plus v4.2, Media Cybernetics, Silver Springs, MD., 1999.
9. Pope, S. B., *Turbulent Flows*, Cambridge University Press, Cambridge, 2000.